nature portfolio

https://doi.org/10.1038/s42256-022-00505-4

Supplementary information

Learning plastic matching of robot dynamics in closed-loop central pattern generators

In the format provided by the authors and unedited

S1. Robot Mechanics

The robot consists of four 'biarticular legs' [12, Fig. 1B] mounted to a carbon fiber compound plate (CFK sandwich, *carbon-vertrieb*). The body structure provides high bending and torsion stiffness at low weight. Each leg is articulated by two brushless outrunner motors (MN7005, *tmotors*). The hip motor is geared through a 1:5 planetary gearbox (RS3505S, *Matex*), the knee motor is geared through a 1:12 one-directional cable drive mechanism to flex the knee joint. The knee extends through the knee spring that tensions during flexion. The knee and ankle joints of the robot are instrumented with rotary encoders (AEAT8800, *Broadcom*). A hall-effect switch (DRV5023, *Texas Instruments*) between the body and femur segment provides a reference to initiate the angle measurements of the hip joints. Hard stops at the robot's knee and ankle joints prevent overextension during stance phase. Four hall-effect current sensors (ACS723, *Alegro Microsystems*) measure input currents to the motor driver boards. The robot is controlled by a Raspberry Pi 4 through a custom-made shield. The shield consists of a SPI GPIO expander (MCP23017, *Microchip* and four tri-state buffers (74HC125, *nexperia*). The shield connects four SPI controlled custom brushless motor drivers [72], the hall switches and the joint encoders to the computer. Two external 12 V 80 A lead batteries supply motors and the computer with power.

Here we focus on motion in the sagittal plane. The robot is therefore constrained to motion in the sagittal plane by a linear rail and lever mechanism that also allows body pitch around the robot's center of mass (COM). The robot walks on an off-the-shelf recreational treadmill (TM500S, *Christopeit*) that is retrofitted with a motor controller (DPCANIE, *amc*). Treadmill speed is measured with a rotary encoder (AEAT8800, *Broadcom*). The robot is connected to the treadmill with a linear rail (SSEB, *Misumi*) and a lever mechanism. The linear rail is equipped with a linear encoder (AS5311, *ams*). The experimental setup can be seen in Figure 1b.

To measure ground contact each foot is equipped with a FootTile sensor [64] connected to a I^2C multiplexer (TCA9548A, *Texas Instruments*). The sensor dome is a half-cylinder with a half-cylinder air cavity that houses the sensor. We do not expect forces in the lateral direction due to the guiding mechanism. Therefore, the sensor domes are laterally symmetric (Figure 1b). As the FootTile sensors are analog pressure sensors, we define a threshold to measure when the sensors are in contact with the ground. The sensors read values between 98.5 and 99 kPa when not in contact with the ground. We define 100 kPa as the contact threshold.

All data on the robot is sampled at 500 Hz except for the FootTile data is sampled at 250 Hz because of limitations in the pressure sensor hardware.

TABLE S1: **Robot parameters**

Parameter	Value
Quadruped robot Morti	
Leg length	408 mm
Body length	350 mm (shoulder - hip)
Width	120 mm (shoulder - shoulder)
Mass	3.6 kg
Hip gear ratio	1:5
Knee gear ratio	1:12
Max. hip torque	6.2 Nm
Max. knee torque	14.9 Nm
Knee cam radius	30 mm
Knee spring stiffness	10.89 $\frac{\mathrm{N}}{\mathrm{mm}}$
Biarticular spring stiffness	9.8 $\frac{\mathrm{N}}{\mathrm{mm}}$
FootTile Sensor	
Dome material	Vytaflex 40
Dome diameter	10 mm
Dome width	10 mm
Sample rate	250 Hz
Resolution	12 bit

S2. CPG

The CPG is described by a system of coupled differential equations:

$$\dot{\phi_j} = \Omega_j \tag{S1}$$

for phase vector

$$\phi = \begin{pmatrix} \phi_{\mathrm{frontLeft}} \\ \phi_{\mathrm{frontRight}} \\ \phi_{\mathrm{hindLeft}} \\ \phi_{\mathrm{hindRight}} \end{pmatrix}$$

where ϕ is the oscillator phase vector and Ω is the angular velocity vector.

$$\dot{\phi_j} = 2\pi f + \sum_{k=1}^{N} \alpha_{\mathrm{dyn},j,k} \cdot \mathbf{C}_{jk} \cdot \sin(\phi_k - \phi_j - \mathbf{\Phi}_{jk}) \tag{S2}$$

where f is the frequency, $\alpha_{\mathrm{dyn},j,k}$ is the conversion constant of the network dynamics between nodes j and k, $\mathbf{C}_{jk}$ is the coupling matrix weight between nodes j and k, $\mathbf{\Phi}_{jk}$ is the desired phase difference matrix value between nodes j and k. All constants are shown in Table S5. With the chosen constants the CPG entrains itself in 1 s which is equivalent to one full gait cycle.

$$\phi_j = \begin{cases} \frac{\phi_j}{2 \cdot D} & \phi_j < 2\pi \cdot D \\ \frac{\phi_j + 2\pi(1-2\cdot D)}{2(1-D)} & else \end{cases} \tag{S3}$$

$$D = \frac{t_{\mathrm{stance}}}{(t_{\mathrm{stance}} + t_{\mathrm{flight}})} \tag{S4}$$

where ϕ_j is the $\mathrm{j^{th}}$ end-effector phase, D is the duty factor, t_{stance} is the duration of stance phase and t_{flight} is the duration of flight phase.

$$\Theta_{\mathrm{hip,des,j}} = \Theta_{\mathrm{hipOffset},j} + \Theta_{\mathrm{hipAmplitude},j} \cdot \cos(\phi_j) \tag{S5}$$

Θ_{hip} is the hip reference trajectory vector, $\Theta_{\mathrm{offset},j}$ is the hip offset and $\Theta_{\mathrm{hipAmplitude},j}$ is the hip amplitude of node j. Depending on the gait symmetry, Θ_{offset} and $\Theta_{\mathrm{hipAmplitude}}$ are also only equal in legs that share the same gait symmetry. For example, in trot, all four legs move symmetrically

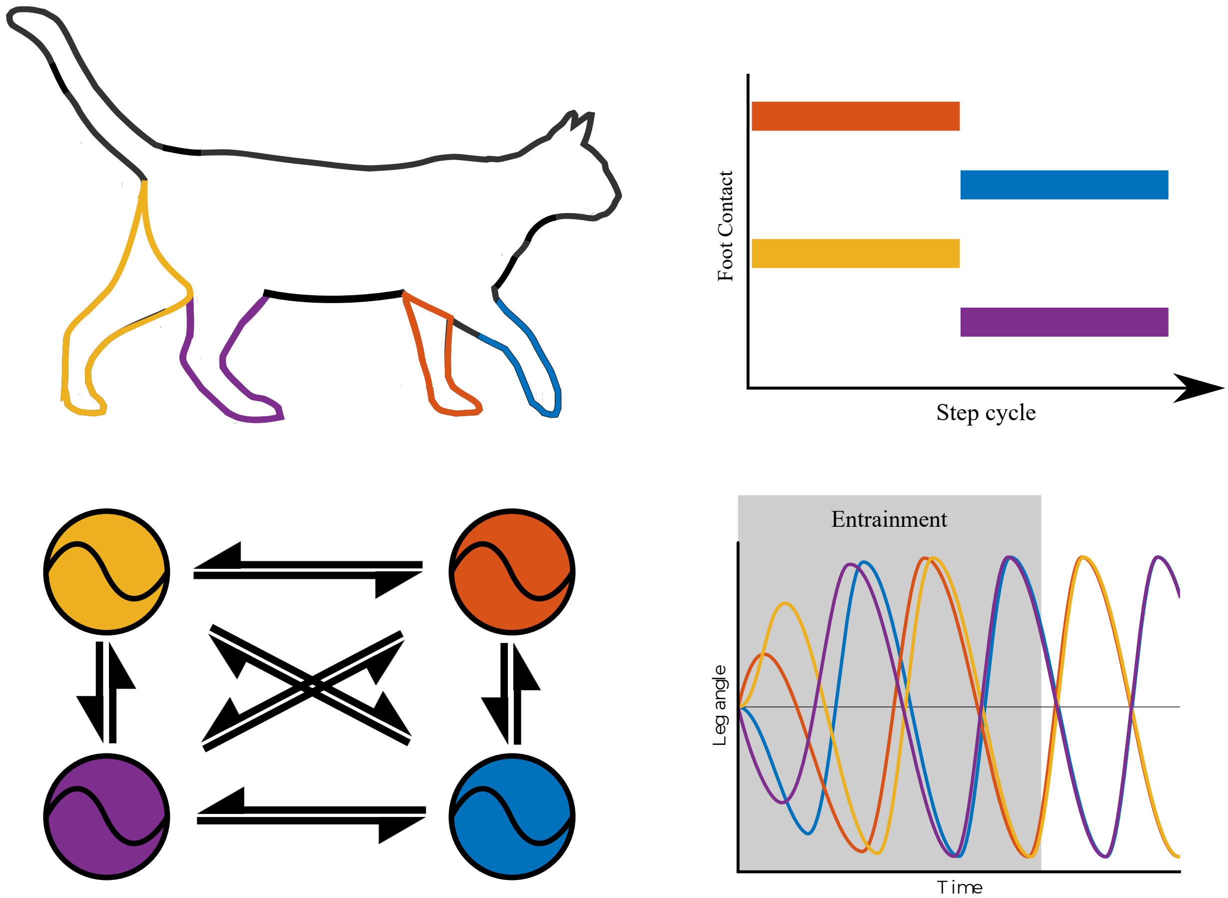

Fig. S1: **Schematic CPG representation.** Each CPG node (bottom left) represents the gait phase of one leg (top left). Through phase differences in between nodes/legs different gaits (top right) can emerge. The coupling dynamics (arrows bottom left) the interplay and mutual influence between nodes

so all hip amplitudes ($\Theta_{\text{hipAmplitude},j}$) are equal, where as in bound only the front legs and the hind legs move symmetrically, also $\Theta_{\text{hipAmplitude},1}$ are only equal in the front and hind.

$$\Theta_{\text{knee,des,j}} = \left(\frac{1}{1+e^{\frac{\phi_j - \phi_{\text{flex}}}{T_{\text{flex}}}}} - \frac{1}{1+e^{\frac{\phi_j - \phi_{\text{ext}}}{T_{\text{ext}}}}} \right) \cdot \Theta_{\text{kneeAmplitude}} + \Theta_{\text{kneeOffset}} \tag{S6}$$

$\Theta_{\text{knee,des}}$ is the knee reference trajectory vector, ϕ_{ext} and ϕ_{flex} are phase shifts for the onset of knee flexion and extension and T_{flex} and T_{ext} are the time constant of the transient flexion and extension behavior.

$$\phi_{\text{kneeShift}} = 2\pi \cdot D + \delta_{\phi,\text{knee}} \cdot (2\pi(1-D)) \tag{S7}$$

$$t_{\text{swing}} = 2\pi - \phi_{\text{kneeShift}} \tag{S8}$$

$$t_{\text{half}} = \frac{t_{\text{swing}}}{\beta} \tag{S9}$$

$$\phi_{\text{flex}} = \phi_{\text{kneeShift}} + \frac{t_{\text{half}} \cdot \beta}{2} \tag{S10}$$

$$\phi_{\text{ext}} = \delta_{\text{overSwing}} - \frac{3 \cdot t_{\text{half}} \cdot \beta}{2} \tag{S11}$$

$$T_{\text{flex}} = T_{\text{ext}} = \frac{t_{\text{swing}}}{2 \cdot \beta} \tag{S12}$$

where $\phi_{\text{kneeShift}}$ is the knee activity onset, $\delta_{\phi,\text{knee}}$ is the desired phase shift between ϕ_j and knee flexion, t_{swing} is the swing duration, t_{half} is the halftime of the transient knee behavior, $\delta_{\text{overSwing}}$ is the shift between ϕ_j and knee extension onset and β is the conversion rate of the transient knee behavior (usually $2 \cdot [5..7] \cdot T_j$). The generated trajectory can be seen in Figure 4. These equations ensure that the whole swing phase is used for knee activity and that both $\Theta_{\text{kneeAmplitude}}$ and $\Theta_{\text{kneeOffset}}$ are reached within one swing

TABLE S2: **CPG parameters as used in Equation S1 - Equation S12.**

Parameter p_m	Symbol	Description
p_0	$\Theta_{\text{hipOffset}}$	Hip offset
p_1	$\Theta_{\text{hipAmplitude}}$	Hip amplitude
p_2	$\Theta_{\text{kneeAmplitude}}$	Knee amplitude
p_3	$\Theta_{\text{kneeOffset}}$	Knee offset
p_4	f	Frequency
p_5	$\delta_{\phi,\text{knee}}$	Knee phase shift
p_6	D	Duty factor
p_7	$\delta_{\text{overSwing}}$	Knee overswing

phase.
All CPG parameters p_m are modeled as a first-order differential equations to ensure smooth transitions to enable online changes of CPG parameters.

$$\dot{p_m} = \alpha_m \cdot (p_{m,\text{des}} - p_m) \tag{S13}$$

where α_m are the conversion rates for the CPG parameters and $p_{m,\text{des}}$ are the desired values for p_m. An example output for four coupled oscillators with their trajectories and a depiction of the CPG parameters described here can be seen in Figure 4. All CPG parameters are shown in Table S2. The coupling matrix C represents a fully, bidirectionally coupled network. Full coupling ensures entrainment of the network for all initial conditions. The coupling matrix $\mathbf{C}$ and desired phase difference matrix $\mathbf{\Phi}$ are shown in Table S4.

A. *Control Structure*

The trajectories generated by the CPG (Equation S5 and Equation S6) are position references for PID-control loops calculating the desired joint motors currents:

$$\begin{aligned} i_{\text{hipMotor}} =& k_p \cdot (\Theta_{\text{hip,des}} - \Theta_{\text{hip}}) \\ &+ k_d \cdot \frac{\mathrm{d}}{\mathrm{d}t}(\Theta_{\text{hip,des}} - \Theta_{\text{hip}}) \\ &+ k_i \cdot \sum_j (\Theta_{\text{hip,des}} - \Theta_{\text{hip}})\Delta t \end{aligned} \tag{S14}$$

where i_{hipMotor} is the desired hip motor current, $k_{\text{p,i,d}}$ are the controller gains and Θ_{hip} is the hip angle.

$$\begin{aligned} i_{\text{feedForward}} =& \frac{c_{\text{spring}} \cdot r_{\text{cam}}^2 \cdot \Theta_{\text{hip}}}{\tau_{\text{m}} \cdot i_{\text{gear}}} \\ i_{\text{kneeMotor}} =& k_p \cdot (\Theta_{\text{knee,des}} - \Theta_{\text{knee}}) \\ &+ k_d \cdot \frac{\mathrm{d}}{\mathrm{d}t}(\Theta_{\text{knee,des}} - \Theta_{\text{knee}}) \\ &+ k_i \cdot \sum_j (\Theta_{\text{knee,des}} - \Theta_{\text{knee}})\Delta t \\ &+ i_{\text{feedForward}} \end{aligned} \tag{S15}$$

where $i_{\text{kneeMotor}}$ is the desired knee motor current, k_{p}, k_{i}, k_{d} are PID controller gains and Θ_{knee} is the knee angle. Additionally the desired knee current contains a feed-forward term, $i_{\text{feedForward}}$, that calculates the required static current to compress the knee spring based on the knee angle where c_{spring} is the knee spring stiffness, r_{cam} is the knee cam radius, τ_{m} is the knee motor torque constant and i_{gear} is the knee gear ratio. The passive knee spring provides passive impedance to the knee joint depending on the knee angle. The feed-forward term compensates the torque the knee spring exerts on the knee joint and reduces the required controller gains to keep the PID controller stable.

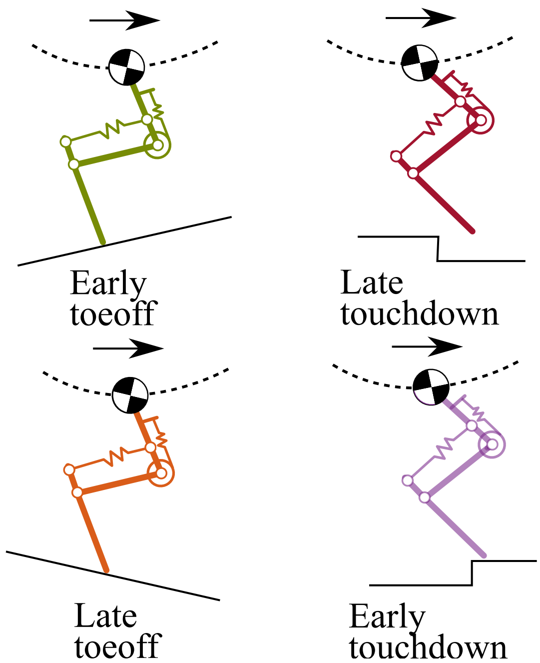

Fig. S2: **Feedback scenarios.** Depiction of four exemplary feedback scenarios where closed loop timing feedback would be active for each feedback mechanism shown in Figure 2d. Late touchdown (top left), early touchdown (top right), late toeoff (bottom left) and early toeoff (bottom right)

S3. Feedback Mechanisms

A. *Late Touchdown r_{LTD}*

The CPG assumes that for $\phi = 0$ the leg is in the forward position and establishes contact with the ground. If there is no ground contact the leg should wait in this position until contact is established. Righetti et al. [35] implemented a phase deceleration during the end of swing phase. In biomechanical studies the phenomenon of swing leg retraction is reported [65] and is also reported in robots [12]. Swing leg retraction describes a period before touchdown, where the leg is already moving backwards but has not yet established ground contact. For this reason, we add a phase shift when $\phi \geq 0$ to achieve contact while allowing overswing in the leg. To achieve acceleration and deceleration in the phase oscillators we use a control term u according to [35] in Equation S2 :

$$\dot{\phi_j} = 2\pi f + \sum_{k=1}^{N} C_{jk} \cdot \sin(\phi - \phi_j - \Phi_{jk}) + u \tag{S16}$$

where

$$\begin{aligned} u =& -(2\pi f + \sum_{k=1}^{N} \alpha_{\text{dyn},j,k} \cdot C_{jk} \cdot \sin(\phi_k - \phi_j - \Phi_{jk})) \\ &\cdot (1 - (\delta_{\text{decay}})^b) \end{aligned} \tag{S17}$$

for b consecutive control loop updates of the CPG dynamics where no contact was established, where $0 \leq \delta_{\text{decay}} \leq 1$ is the base of the exponential function that decays $\dot{\phi}_j$ to zero in k steps, to decelerate the oscillator node. This deceleration can be seen in Figure 4, in the top graphs where the slope of the oscillator phase decreases (red) until contact (gray shaded area) is established. For re-entrainment after one phase is decelerated "out of phase" we utilize the inherent coupling dynamics of the network Equation S2. Based on the weight matrix α_{dyn}, the dynamics of the network can be adjusted to enforce entrainment of the network well within one stride cycle of the robot.

B. Late Toeoff r_{LTO}

The same mechanism for late touchdown can also be applied for late toeoff. At the end of stance phase, the leg waits until the end of ground contact before initiating swing phase. This waiting period effectively also closes the loop on the timing of the knee trajectory as the knee and hip trajectories are directly coupled through the same phase reference. The late toeoff mechanism described here, however, only works for gaits with flight phase as the legs otherwise never lift off the ground because of double support during stance phase. In this case, swing phase has to be initiated through a feed-forward timing of knee flexion. As shown in the results section, the late toeoff mechanism was not used for phase deceleration as the double stance phase of the robot prevents the legs to disengage from the ground completely and thereby prevents feedback-driven knee flexion. In Righetti et. al. [35] this mechanism was implemented successfully and is therefore also included here. For this study, we record the mismatch stemming from late toeoff but do not trigger the phase delay mechanism.

C. Early Touchdown r_{ETD}

During swing phase the legs can hit the ground prematurely, resulting in the robot stumbling. The perturbation comes from swinging the leg forwards into the ground and at the same time extending the knee. We implement a feedback loop that decreases this parasitic impact. During swing phase (Figure 2d yellow) if the leg hits the ground prematurely we want to flex the knee by an additional 5° to create more ground clearance and at the same time stop the forward swinging of the leg. We therefore disable the hip motor on impact and at the same time increase the knee flexion.

$$\Theta_{\text{knee,j}} = \Theta_{\text{knee,des,j}} + 5^\circ \cdot \exp^{-(\phi_j(r_{\text{ETD}}) - /tau} \tag{S18}$$

where $\Theta_{\text{knee,des,j}}$ is the nominal knee trajectory without feedback, $\phi_j(r_{\text{ETD}})$ is the respective CPG node phase when feedback is active and τ is the decay rate so the knee pullup reflex decays until the end of stance phase.
The switched-off hip motor allows us to leverage the elastic leg behavior in leg length as well as leg angle direction that we presented in our previous work [12]. Impact energy that will be introduced through the premature foot impact during early touchdown will be stored in the knee and biarticular spring and will not destabilize the robot. The controller can therefore take advantage of the passive dynamic behavior of the leg as well as its elastic capabilities to improve stability. After the next phase transition to 2π the knee trajectory goes back to its normal behavior. Through the CPG coupling dynamics as well as the smoothing equations (Equation S13) the trajectory will converge back to the CPG's limit cycle without the necessity for additional feedback.

D. Early Toeoff r_{ETO}

If the leg loses contact to the ground during stance phase we want the knee to start flexing earlier to prevent further ground contact. To do so we recalculate $\Theta_{\text{kneeShift}}$ (Equation S7) from the time of early toeoff to initiate early flexion and reconfigure the knee trajectory to fit the feedback timing. This mechanism provides enough ground clearance to swing the leg backward to its turning point and forwards during flight phase.

S4. Cost function

The plasticity term minimizes the use of feedback by matching control dynamics to the robot's natural dynamics.

$$J_{\text{feedback}} = \frac{1}{f \cdot n \cdot T} \sum_{n=0}^{4} \sum_{t=0}^{T} r_{\text{ETO}} + r_{\text{ETD}} + r_{\text{LTO}} + r_{\text{LTD}} \tag{S19}$$

where J_{feedback} is the average percentage of active feedback per step and leg, n is the number of legs, T is the evaluation time and r_{ETO}, r_{ETD} ,r_{LTO},r_{LTD} are the time vectors when the specific feedback was active for each leg.
To evaluate locomotion performance we use body position as we want the robot to cover as much distance as possible for a given CPG parameter set.

$$J_{\text{distance}} = \frac{1}{x_{\text{body}}} \tag{S20}$$

where x_{body} is the center of mass position in walking direction. Note that the COM position is inverted because of the minimization approach of *gp_minimize*
The contact cost term minimizes the amount of additional contact state switches (steps) per stride cycle

$$J_{\text{contact}} = \frac{1}{f \cdot n \cdot T} \sum_{n=0}^{4} \sum_{t=0}^{T} \left(\left\| \frac{\text{d}}{\text{dt}} \text{contact} \right\| > 0 \right) \tag{S21}$$

where J_{contact} is the mean amount of flight-stance changes per step, n is the number of legs, t is time, T is the evaluation duration and contact is the contact sensor data matrix for all four legs.
The periodicity term minimizes non-periodic behavior of the robot to make sure the performance of the robot does not come from undesired behavior like non-periodic jumps or skips. To do so we calculate the average distance of the maxima from the autocorrelation of the pitch angle. The pitch angle is convoluted with itself to obtain the frequency spectrum of the body pitch angle. We then compare this frequency with the actual CPG frequency, by calculating the standard deviation to determine how well the CPG and the robot's

TABLE S3: **Cost terms with estimated range and weights**

Cost factors J_j	Description	Range	Weight w_j
J_{feedback}	plasticity	0 - 1	6
J_{distance}	performance	0 - $\frac{1}{10}$	9
$J_{\text{periodicity}}$	periodic behavior	0 - 2	2
J_{contact}	contact phases	0 - 5	0.5
J_{pitch}	body pitch	0 - 10	$\frac{180^\circ}{5 \cdot \pi}$

passive dynamics match. The standard deviation provides a good measure of the variation in the oscillatory behavior and is used to characterize how well the CPG dynamics fit the mechanical dynamics of the robot.

$$\begin{aligned} S_{\text{pitch}} &= \alpha_{\text{pitch}} * \alpha_{\text{pitch}} \\ f_{\text{bodyPitch}} &= \|\max S_{\text{pitch}}\| \\ J_{\text{periodicity}} &= \sqrt{\frac{1}{N}\left(f_{\text{bodyPitch}} - f_{\text{cpg}}\right)^2} \end{aligned} \tag{S22}$$

(S23)

where S_{pitch} is the frequency spectrum of the body pitch signal α_{pitch}, $f_{\text{bodyPitch}}$ is the frequency of the body pitch measurement, $J_{\text{periodicity}}$ is the standard deviation of the periodicity measure and f_{cpg} is the commanded CPG frequency. The body pitch term minimizes the body rotation of the robot during locomotion and ensures stable gaits and energy efficient behavior.

$$J_{\text{pitch}} = \|\max(\alpha_{\text{pitch}}) - \min(\alpha_{\text{pitch}})\| \tag{S24}$$

where J_{pitch} is the mean body pitch amplitude of the robot. It is calculated as the difference between mean minimum and mean maximum pitch angle of all strides during one iteration. The cost function is then calculated as the weighted sum of all the cost terms shown in Table S3. Should the robot fall before the entrainment period is over or it moves backwards, the robot is costed a high penalty (100) for failure. If the robot falls after the entrainment time, the performance until that point is evaluated. Here the distance cost J_{distance} is used as a punishing reinforcement by degrading the cost signal. The cost is calculated as:

$$J = \sum_{j=1}^{N} w_j \cdot J_j \tag{S25}$$

where J is the cost signal, w_j are the cost weights and J_j are the cost factors in Equation 3 to Equation 7

S5. Toy Example

To elucidate the matching of natural and controller frequency we implement a simple mathematical pendulum Figure S3. It is a representation for a system with strong natural dynamics in its natural oscillation frequency governed by the pendulum length and mass. The pendulum is actuated by a torque τ to oscillate harmonically with a given frequency f through a simple PD-controller. Based on the enforced oscillation frequency f from the motor compared to the natural frequency f_n of the pendulum it is easy to show the effect of mismatched frequencies. For values of f close to the natural frequency, the required power reduces. Because the frequency of the control pattern matches the natural behavior of the pendulum, the system requires less control effort and motor power to achieve the desired motion.

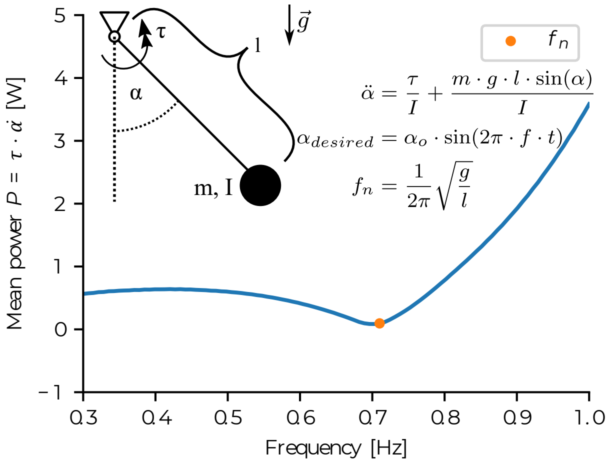

Fig. S3: **Pendulum toy example.** Toy example of the effects of matching control frequency and natural frequency in a physical pendulum. The closer the control pattern frequency matches the natural frequency of the system (part of the natural dynamics) the lower the required power is because the controller can leverage the behavior of the natural dynamics. Parameters are: $m = 1\,\text{kg}$, $l = 0.5\,\text{m}$, $\alpha_0 = 30^\circ$, $k_{\text{p,motor}} = 50$, $k_{\text{d,motor}} = 0.7$

While this toy example only features simple dynamics and does not include effects like nonlinear impedance and switching dynamics, it can still demonstrate, how leveraging the natural dynamics of a system in the control pattern can improve the energy efficiency. If a locomotion controller can take advantage of the natural dynamics that are designed to aid locomotion passively, the same power requirement reduction will show in more complex walking systems.

$$\begin{aligned} \ddot{\alpha} &= \frac{\tau}{I} + \frac{m \cdot g \cdot l \cdot \sin(\alpha)}{I} \\ \alpha_{\text{desired}} &= \alpha_0 \cdot \sin(2\pi \cdot f \cdot t) \\ \tau &= k_p \cdot (\alpha - \alpha_{\text{desired}}) + k_d \cdot \frac{\alpha - \alpha_{\text{desired}}}{\Delta t} \\ f_n &= \frac{1}{2\pi}\sqrt{\frac{g}{l}} \\ P &= \tau \cdot \dot{\alpha} \end{aligned} \tag{S26}$$

where α is the pendulum angle, τ is the motor torque, m is mass, g is gravitational acceleration, l is the pendulum length, I is the pendulum inertia, α_{desired} is the desired pendulum angle, α_0 is the oscillation amplitude, f is the oscillation frequency, t is time, k_{d} and k_{d} are the PD controller gains and P is motor power. Because this matching is non-trivial in our robotic walking machine due to highly nonlinear impedance behavior leading to nonlinear Eigenmodes and underactuation, a mathematical formulation is not possible. Alternatively, a data-driven approach can be used to approximate the performance landscape of the frequency relationship.

TABLE S4: **Coupling matrix C and desired phase difference matrices Φ for different gaits**

$$\mathbf{C} = \begin{bmatrix} 0 & 1 & 1 & 1 \\ 1 & 0 & 1 & 1 \\ 1 & 1 & 0 & 1 \\ 1 & 1 & 1 & 0 \end{bmatrix} \tag{S27}$$

$$\mathbf{\Phi}_{\text{trot}} = \begin{bmatrix} 0 & -\pi & -\pi & 0 \\ \pi & 0 & 0 & \pi \\ \pi & 0 & 0 & \pi \\ 0 & -\pi & -\pi & 0 \end{bmatrix} \tag{S28}$$

$$\mathbf{\Phi}_{\text{bound}} = \begin{bmatrix} 0 & 0 & -\pi & -\pi \\ 0 & 0 & -\pi & -\pi \\ \pi & \pi & 0 & 0 \\ \pi & \pi & 0 & 0 \end{bmatrix} \tag{S29}$$

$$\mathbf{\Phi}_{\text{pace}} = \begin{bmatrix} 0 & -\pi & 0 & -\pi \\ \pi & 0 & \pi & \pi \\ 0 & -\pi & 0 & -\pi \\ \pi & -\pi & \pi & 0 \end{bmatrix} \tag{S30}$$

$$\mathbf{\Phi}_{\text{walk}} = \begin{bmatrix} 0 & -\frac{\pi}{2} & -\pi & -\frac{3\pi}{2} \\ \frac{\pi}{2} & 0 & -\frac{\pi}{2} & -\pi \\ \pi & \frac{\pi}{2} & 0 & -\frac{\pi}{2} \\ \frac{3\pi}{2} & \pi & \frac{\pi}{2} & 0 \end{bmatrix} \tag{S31}$$

TABLE S5: **Conversion factors**

Conversion factor	Value
$\alpha_{\text{hipOffset}}$	4
$\alpha_{\text{hipAmplitude}}$	4
$\alpha_{\text{kneeAmplitude}}$	4
$\alpha_{\phi,\text{knee}}$	4
$\alpha_{\text{overSwing}}$	4
$\alpha_{\text{DutyFactor}}$	3
$\alpha_{\text{dyn,i,j}}$	2
α_{f}	1
$\alpha_{\text{phaseDifference}}$	1

S6. CPG MATRICES

Table S4 shows the coupling matrix $\mathbf{C}$ that defines the connections between CPG nodes for ϕ as in Equation S1. $\mathbf{\Phi}$ describes the desired phase differences between CPG nodes. Table S5 describes the conversion factors used in Equation S2 and Equation S13. With these factors, the convergence of the smooth transitions can be accelerated when a CPG parameter is changed. The CPG conversion factors are chosen in a way that ensures changes in trajectory-related parameters to change within one stride of the robot. Factors for frequency (α_{f}) and phase difference ($\alpha_{\text{phaseDifference}}$) are lower, so that transitions take several steps to change to keep the robot behavior stable.

S7. OPTIMIZATION RESULTS

Table S6 shows the comparison of optimization results from simulation as well as the parameters of the most successful hardware experiment.

S8. SUPPLEMENTARY PLOTS

Figure S4 shows the gait pattern of the most successful hardware experiment. The contact data obtained from the FootTile sensors is averaged over 10 steps and displayed over a step cycle. The gait shows a slight asymmetry between legs that should contact at the same time due to minimal differences in the hip reference angles. The hind legs also show a short time where the foot loses contact right after touchdown. This can also be seen in the provided high-speed video and is due to the perturbations stemming from body pitch that are not captured in the CPG equations.

TABLE S6: **Optimization results**

Parameter	Simulation Results	Hardware Results	Optimization Range
$\Theta_{\text{hipOffset}}$	0 °	-0.45°	[-5,5]°
$\Theta_{\text{hipAmplitude}}$	16 °	15°	[5,20]°
$\Theta_{\text{kneeAmplitude}}$	30 °	30°	[30]°
$\delta_{\phi,\text{knee}}$	0.1 [rad]	0.8 [rad]	[-0.2π,0.2π]
$\delta_{\text{overSwing}}$	0.13 [rad]	0.11 [rad]	[-0.2π,0.2π]
D_{front}	0.56	0.55	[0.3,0.6]
D_{hind}	0.56	0.55	[0.3,0.6]

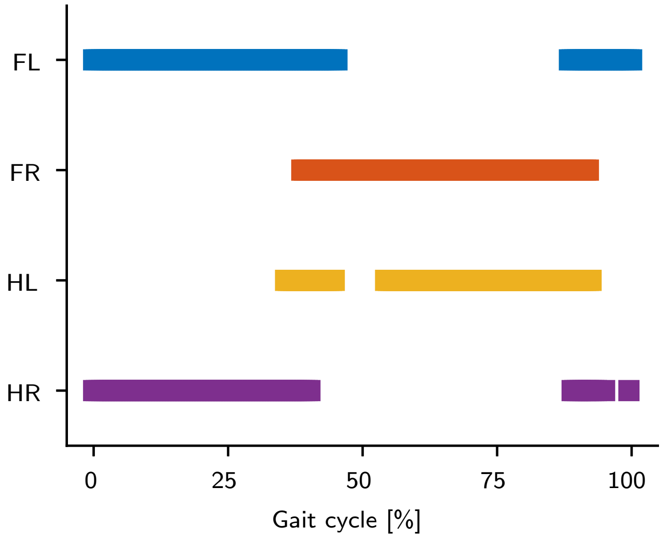

Fig. S4: **Gait pattern.** Emerging gait pattern after optimization in hardware. The gait that emerged is a trot gait. Data shown here is averaged over 10 steps. In both hind legs a small fraction of time is visible where the legs lose contact to the ground due to the pitching body.

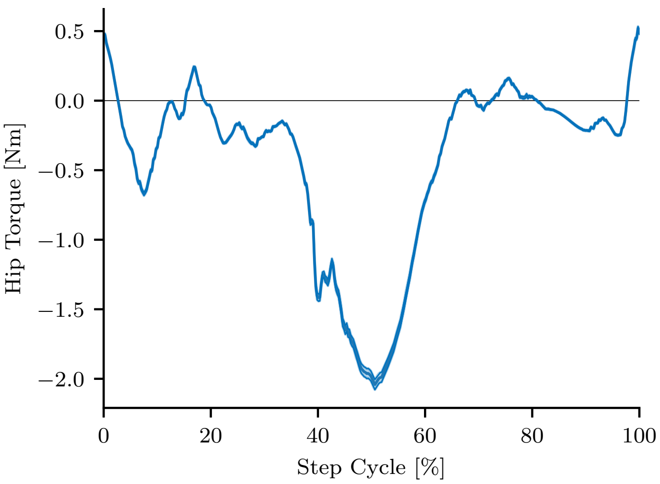

Fig. S5: **Torque pattern.** Torque Pattern of the front-left hip motor during one of the hardware experiments. Data is averaged over 22 steps and shown with 95% confidence interval.